Supplemental Document

Biomedical Optics EXPRESS

Maximum a posteriori signal recovery for optical coherence tomography angiography image generation and denoising: supplement

LENNART HUSVOGT,[1,2,*] STEFAN B. PLONER,[1] SIYU CHEN,[2] DANIEL STROMER,[1,2] JULIA SCHOTTENHAMML,[1] A. YASIN ALIBHAI,[3] ERIC MOULT,[2] NADIA K. WAHEED,[3] JAMES G. FUJIMOTO,[2] AND ANDREAS MAIER[1]

[1] *Pattern Recognition Lab, Friedrich-Alexander-Universität Erlangen-Nürnberg, Germany*
[2] *Research Laboratory of Electronics, Massachusetts Institute of Technology, Cambridge, MA 02139, USA*
[3] *New England Eye Center, Tufts School of Medicine, Boston, MA 02111, USA*
[*] *lennart.husvogt@fau.de*

Supplement DOI: https://doi.org/10.6084/m9.figshare.13120001

Parent Article DOI: https://doi.org/10.1364/BOE.408903

Maximum A Posteriori Signal Recovery for Optical Coherence Tomography Angiography Image Generation and Denoising: supplemental document

This supplementary document contains a section explaining the relationship of the presented reconstrucion algorithm to compressed sensing, the maximum likelihood estimate for speckle variance, and reconstruction results for OCTA using speckle variance.

1. RELATIONSHIP WITH COMPRESSED SENSING

The presented reconstruction algorithm is based on Bayesian statistics, but can be related to compressed sensing (CS) when a regularizer is used which enforces sparsity, such as wavelet thresholding or total variation minimization. The following description should be read as a supplementary to section 2.1 in the main paper.

CS has already been used in the past for the generation of structural OCT images [1]. Liu et al. and Mohan et al. demonstrated the use of CS for spectral domain OCT to reduce the amount of k-space samples that need to be acquired [2–4]. Young et al. employed CS for real-time volumetric imaging [5] while Fang et al. performed so called multiscale sparsity-based tomographic denoising [6, 7]. This CS method allows the denoising of spectral domain OCT data using custom scan patterns. Zhang et al. also utilized CS by using a linear mask in k-space for subsampling which reduces the number of samples necessary for OCT signal generation [8]. Xu et al. implemented a denosing method for spectral domain OCT also based on CS and achieved real-time capability [9–11].

The challenge which CS addresses, is the case where the system matrix $\mathbf{A}$ is a linear mapping with $M < N$. In that case, $\mathbf{A}$ is being underdetermined which leads to an infinite number of possible solutions for $\mathbf{X}$. CS allows to find solutions in this case by exploiting sparsity of $\mathbf{X}$ in a certain basis. A good example for a different basis used in CS are the coefficients of a wavelet transform. $\mathbf{X}$ is then called k-sparse when it has k non-zero entries in that basis.

In addition to that, based on the iterative hard thresholding algorithm, Blumensath generalized CS for cases in which $\mathbf{A}$ is non-linear and non-invertible and showed that under certain conditions the Landweber iteration can also be used here [5, 6].

2. MAXIMUM LIKELIHOOD ESTIMATE FOR SPECKLE VARIANCE

Speckle variance is defined as the variance of the amplitude values y_1 to y_N [12]

$$x = \frac{1}{N} \sum_{n=1}^{N} (y_i - \mu)^2 \ , \tag{S1}$$

with μ being the mean of y_1 to y_N. This can be shown through a maximum likelihood estimation. Under the assumption that y_i is normally distributed and

$$\mathrm{P}\left(y_i \middle| \mu, \sigma^2 = x\right) \tag{S2}$$

being the probability of y_i being measured given μ and $\sigma^2 = x$, is

$$L_{\mathrm{SV}} = \prod_{i=1}^{N} \mathrm{P}\left(y_i|\mu, x\right) = \prod_{i=1}^{N} \frac{1}{\sqrt{2\pi x}} \exp\left(-\frac{(y_i - \mu)^2}{2x}\right) \tag{S3}$$

the likelihood of all y_i. Choosing μ and x to maximize $\log L_{\mathrm{SV}}$ yields

$$\underset{\mu,x}{\arg\max} \log L_{\mathrm{SV}} = \underset{\mu,x_{\mathrm{SV}}}{\arg\max}\, N \cdot \log \frac{1}{\sqrt{2\pi x}} - \sum_{i=1}^{N} \frac{\left(a_i - \mu^2\right)}{2x} \ . \tag{S4}$$

Note that working with the log-likelihood simplifies the derivation below. In order to find the maximum we look at the first order derivative with respect to $x_{\mathrm{SV},\mathbf{p}}$ and set it to 0

$$\frac{d \log L_{\mathrm{SV}}}{dx} = \frac{-N \cdot x + \sum_{i=1}^{N} (a_i - \mu)^2}{2x^2} . \tag{S5}$$

This shows that the maximum is located at

$$x = \frac{1}{N} \sum_{i=1}^{N} (y_i - \mu)^2 , \tag{S6}$$

which is the function for SV.

3. RESULTS

Fig. S1 shows peak signal-to-noise ratio (PSNR) and structural similarity (SSIM) plots for the reconstruction results, while Fig. S2 shows the 98th percentile en face projections of the reconstructed volumes.

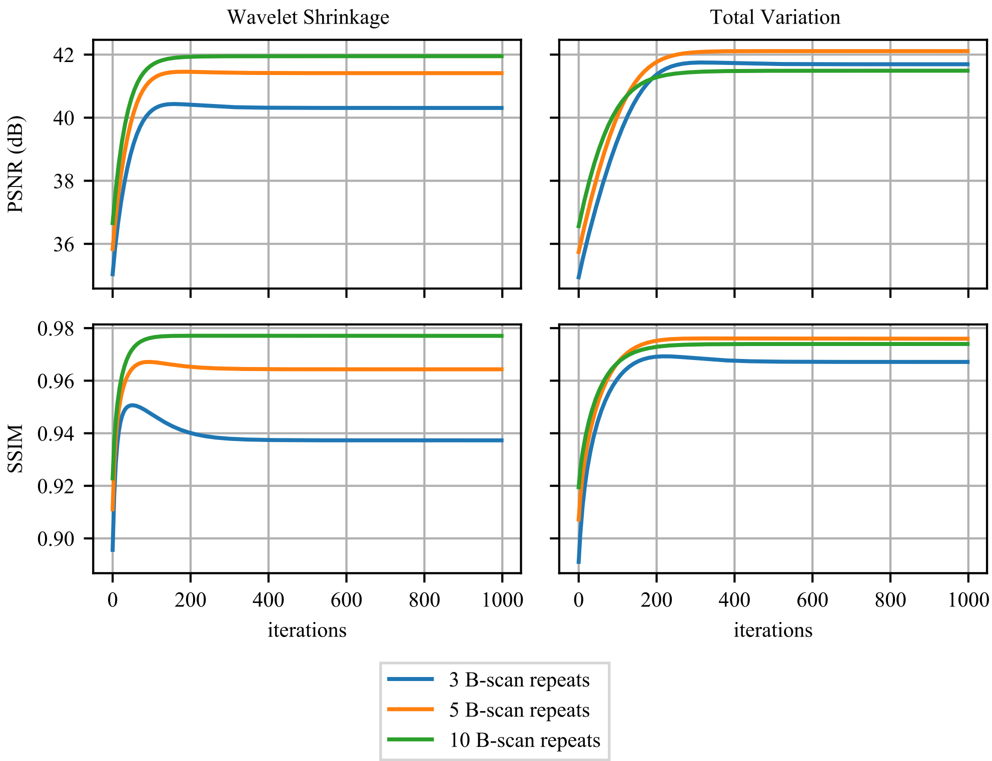

Fig. S1. Peak signal-to-noise ratio (PSNR) and structural similarity (SSIM) during reconstruction. The color indicates whether three, five, or ten repeated B-scans were used for reconstruction. The rows show PSNR for amplitude decorrelation and interframe variance, the columns indicate the regularizer.

REFERENCES

1. E. J. Candès and M. Wakin, "An Introduction To Compressive Sampling," IEEE Signal Process. Mag. (2008).
2. M. Lustig, D. Donoho, and J. M. Pauly, "Sparse MRI: The application of compressed sensing for rapid MR imaging," Magn. Reson. Medicine (2007).
3. E. Y. Sidky and X. Pan, "Image reconstruction in circular cone-beam computed tomography by constrained, total-variation minimization," Phys. Medicine Biol. **53**, 4777–4807 (2008).

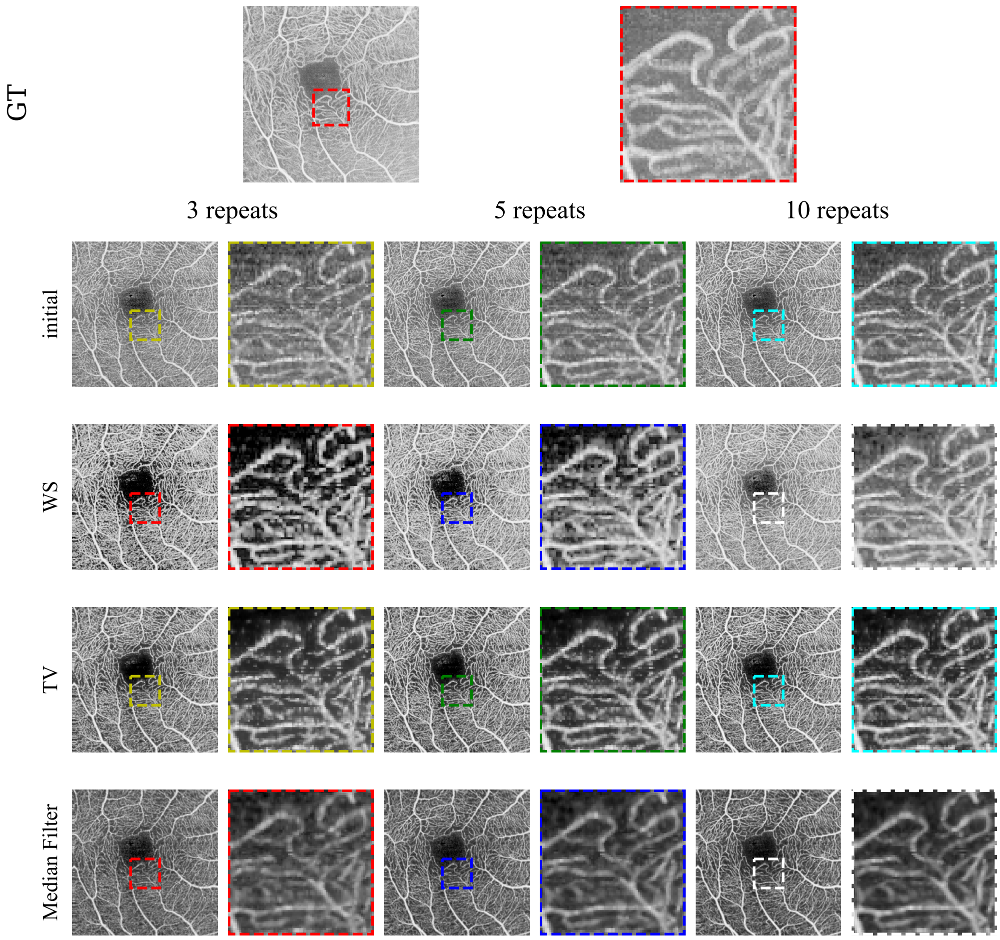

Fig. S2. En face projections of the GT and reconstruction results. More detailed areas are shown in enlargements next to the en face images. Rows show initial OCTA, wavelet shrinkage, total variation reconstructions, and median filter for comparison. Columns are grouped by the number of scan repeats used.

4. H. Wu, A. Maier, R. Fahrig, and J. Hornegger, "Spatial-temporal total variation regularization (STTVR) for 4D-CT reconstruction," in *Medical Imaging 2012: Physics of Medical Imaging,* vol. 8313 N. J. Pelc, R. M. Nishikawa, and B. R. Whiting, eds. (International Society for Optics and Photonics, 2012).
5. M. Amrehn, A. Maier, F. Dennerlein, and J. Hornegger, "Portability of TV-Regularized Reconstruction Parameters to Varying Data Sets," in *Bildverarbeitung für die Medizin 2015,* H. Handels, T. M. Deserno, H.-P. Meinzer, and T. Tolxdorff, eds. (Springer Vieweg, Berlin, Heidelberg, Berlin, Heidelberg, 2015), pp. 131–136.
6. D. Stromer, M. Amrehn, Y. Huang, P. Kugler, S. Bauer, G. Lauritsch, and A. Maier, "Comparison of SART and ETV reconstruction for increased C-arm CT volume coverage by proper detector rotation in liver imaging," in *2016 IEEE 13th International Symposium on Biomedical Imaging (ISBI),* (IEEE, 2016), pp. 589–592.
7. Y. Huang, G. Lauritsch, M. Amrehn, O. Taubmann, V. Haase, D. Stromer, X. Huang, and A. Maier, "Image Quality Analysis of Limited Angle Tomography Using the Shift-Variant Data Loss Model," in *Bildverarbeitung für die Medizin 2016,* T. Tolxdorff, T. M. Deserno, H. Handels, and H.-P. Meinzer, eds. (Springer Vieweg, Berlin, Heidelberg, Berlin, Heidelberg, 2016), pp. 277–282.
8. A. Wong, A. Mishra, K. Bizheva, and D. A. Clausi, "General Bayesian estimation for speckle noise reduction in optical coherence tomography retinal imagery," Opt. Express **18**, 8338 (2010).
9. X. Liu and J. U. Kang, "Compressive SD-OCT: the application of compressed sensing in spectral domain optical coherence tomography," Opt. Express **18**, 22010–22019 (2010).
10. X. Liu and J. U. Kang, "Sparse OCT: optimizing compressed sensing in spectral domain optical coherence tomography," in *Proc. SPIE,* vol. 7904 J.-A. Conchello, C. J. Cogswell, T. Wilson, and T. G. Brown, eds. (International Society for Optics and Photonics, 2011).
11. N. Mohan, I. Stojanovic, W. C. Karl, B. E. A. Saleh, and M. C. Teich, "Compressed sensing in optical coherence tomography," in *Proc. SPIE,* vol. 7570 J.-A. Conchello, C. J. Cogswell, T. Wilson, and T. G. Brown, eds. (International Society for Optics and Photonics, 2010).
12. S. B. Ploner, C. Riess, J. Schottenhamml, E. M. Moult, N. K. Waheed, J. G. Fujimoto, and A. Maier, "A Joint Probabilistic Model for Speckle Variance, Amplitude Decorrelation and Interframe Variance (IFV) Optical Coherence Tomography Angiography," in *Bildverarbeitung für die Medizin 2018,* A. Maier, T. M. Deserno, H. Handels, K. H. Maier-Hein, C. Palm, and T. Tolxdorff, eds. (Springer Berlin Heidelberg, Berlin, Heidelberg, 2018), 211279, pp. 98–102.